LASER INDUCED DAMAGE THRESHOLD OF SILICON WITH NATIVE AND ARTIFICIAL SiO_2 LAYER

JURAJ SLADEK[1,2], INAM M. MIRZA[1]

1) HiLASE Centrum, Institute of Physics CAS, Dolni Brezany, Czech Republic

2) Department of Solid State Engineering, Faculty of Nuclear Sciences and Physical Engineering, Czech Technical University in Prague, Prague, Czech Republic

DOI: 10.17973/MMSJ.2019_12_2019103

juraj.sladek@hilase.cz

Spot size measurements of a 260 fs, 1030 nm focused spatially Gaussian pulsed laser beam were performed on a Silicon surface with native and thermally grown SiO_2 layers using a widely known method of evaluating laser beam energy dependent damage area. Single pulse laser induced damage thresholds of both samples were also measured. Modification of the thermally grown SiO_2 layer was analyzed in detail using optical, confocal and scanning electron microscopy. Restrictions in Gaussian beam spot size measurements on the samples with transparent coatings and several observable thresholds are discussed.

KEYWORDS

ultra-short laser ablation, laser spot size, silicon damage threshold, Gaussian beam, SiO_2 thin film

1 INTRODUCTION

Efficient and successful laser processing of materials requires a precise control of processing parameters, especially laser energy fluence. Therefore, an accurate knowledge of the beam spot size is essential for this purpose. In some cases, it is not possible to use a digital camera-based beam profiler. Either it is not readily available, or more often, the location of a tightly focused beam is not reachable by such a device. Measurements of the beam energy dependence of the damaged area ($1/e^2$ criteria) are widely used in this case [Liu 1982], often utilizing a silicon wafer as a target material. This is due to its high-quality polished surface (typically few nm for commercial Si wafers) and well-known infrared (IR) femtosecond (fs) laser-matter interaction physics [Bonse 2001, Gnilitskyi 2016]. Multiple studies focused on ablation mechanisms and precise removal of up to a few hundred nanometers (nm) SiO_2 layer from the Si wafer have been performed with ns [Mangersnes 2010], ps [Herman 2009], but mostly by fs laser pulses [Rapp 2013, Rapp 2014, Rublack 2011a, McDonald 2007]. There is also a strong dependence of the ablation mechanisms on wavelength [Hermann 2010], pulse duration [Rublack 2011b] and layer thickness [Hermann 2010]. The laser beam size in the focal range was either characterized prior to sample irradiation using CCD beam profiler [Rublack 2011a, Rublack 2011b], or measured using the method described by Liu [Liu 1982] on a Si wafer covered by a hundred nm SiO_2 layer. Left unreported was the effect of a hundreds of nm thick thermally grown oxide layer on the surface of Si wafer on laser beam spot size measurements. In the present work, we have performed systematic studies of spot size measurements of focused IR, fs pulses on both Si with a few nm native oxide layer, that forms on the Si wafer whenever the wafer is exposed to air under ambient conditions, and ~300 nm thermally grown oxide layer. We demonstrate that the thick surface oxide layer significantly effects the spot size measurements for regimes with higher modification thresholds. We also present single pulse threshold fluences for observed laser induced threshold processes on sample surface, particularly for amorphization, melting, ablation of Si and complete removal of oxide layer (Fig. 1a,b).

2 EXPERIMENTAL METHODS

Experiments were carried out using a commercial laser system (PHAROS, Light Conversion), with a pulse duration of 260 fs and 1030 nm central wavelength. A repetition rate of 50 kHz and maximum pulse energy of 120 µJ was set for our experiment. A sample was placed on an XYZ stage, with manual z motion and a galvanometric scanner (ScanCube IV, Scanlab), positioning the beam across the sample surface. Linearly polarized laser pulses were precisely focused onto the sample surface using a f-theta lens (f = 163 mm). The theoretical resulting $1/e^2$ beam diameter, at the beam focus was 26 µm. Two silicon samples were used: n-doped silicon wafer with thickness of 0.5 mm with just a native surface oxide layer in order of a few nm (~4 nm [Zhang 2010]) as often used in industry and a 0.5 mm thick Si wafer with 300 nm thermal oxide layer.

The laser beam pulse energy was controlled by careful rotation of a lambda half-wave plate in combination with a Glan—Taylor polarizing prism. In all cases, the laser power was measured right after the focusing lens using a thermopile-based sensor (Ophir). The laser pulse energy was obtained by dividing average laser power by the corresponding repetition rate.

In damage threshold measurements, it is essential to keep the sample surface as clean as possible, since the presence of any scratches, dust and ablation particles or other polluting instances behave as scattering and absorption centers and may locally damage the surrounding material. Therefore, both samples were cleaned prior to irradiation by optical tissues wetted by acetone and subsequently methanol, both of optical purity. The irradiation spots were spaced 200 µm apart in order to avoid ablative materials coating interfering with the subsequent pulse.

Laser irradiated spots on the sample surface were studied by several microscopic techniques, namely optical (Olympus BX42), confocal laser scanning (Olympus OLS5000), scanning electron microscope (SEM) (FEI Phenom) and atomic force microscope (AFM) (Xplora-Nano, Horiba scientific) operated in tapping mode. Whereas the SEM and AFM were used to study high resolution surface topography of irradiated spots, while the optical microscopy was used to reveal silicon modification under the 300 nm SiO_2 layer for irradiation regimes below the damage threshold fluence of thick oxide layer.

To determine the damage threshold and beam spot size (defined as $2\omega_0$), we measured the diameter D of a modified region with relation to its specific pulse energy. For a spatially Gaussian laser beam a relation between squared diameter D of modified area and pulse peak fluence $F_0 = 2.E_{pulse}/\pi\omega_0^2$ is given by [Liu 1982]:

$$D^2 = 2.\omega_0^2.\ln\left(\frac{F_0}{F_{th}}\right), \quad (1)$$

where ω_0 denotes the $1/e^2$ radius of Gaussian beam in the focal plane and F_{th} is the searched threshold fluence for a given process (Fig. 1c). Spatial profile of our laser beam was Gaussian with $M^2 < 1.15$, thereby justifying the use of this method for data

evaluation. To combat issues of slightly elliptical pulses, the area A of modification was used to define D by the following formula

$$D^2 = \frac{4A}{\pi}. \quad (2)$$

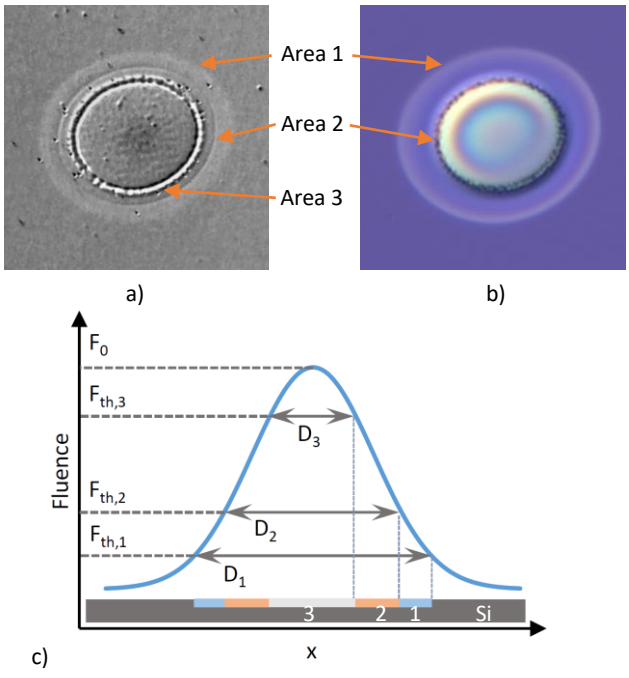

Figure 1. Optical microscope images of typical laser induced damage spots on silicon with native a) (grayscale) and thermally grown oxide layers b). Three different modification areas with damage threshold fluences F_{th} can be distinguished in a). These are illustrated in c) for a spatially Gaussian pulse with peak fluence F_0. Sizes of the outermost visible modified regions in a) and b) are 22 and 20 µm respectively. Marked areas in a) and b) do not correspond to the same modification processes.

3 RESULTS AND DISCUSSION

3.1 Measurement of thresholds

Damage threshold and spot size measurements based on the beam energy dependence of the damaged area requires a material exhibiting sharp threshold process [Liu 1982]. Based on observations in Fig. 1a-b, several such thresholds may co-exist. Despite of being a widely used method, there is little information about how to choose a correct threshold process and what are the effects of thin surface layers. Therefore, we chose three threshold processes on each sample and measured corresponding threshold fluences and resulting spot size values. In the case of silicon with a native oxide layer, we chose to measure three areas. The edge of first area visible as the border between unaffected surface and onset of material amorphization, a region defined by a thin line between amorphization and melting and inner melting ring (see Fig. 1a), which will be referenced to as Area 1, 2 and 3 respectively. Threshold processes considered in the case of silicon with 300 nm oxide layer includes an outer amorphization edge, melting connected with onset of oxide layer blistering and secondary crater creation in the middle part of ablation spots. These will also be referred to as Area 1, 2 and 3 respectively (Fig. 1b).

Outer edges of modification areas were measured from optical, confocal and SEM microscope images. Measured data of the damaged area diameter (2) dependence on beam energy are presented in semi-logarithmic graphs in Fig. 3 for silicon with native oxide layer. Whilst, Fig. 4 demonstrates this for the silicon with a thermally grown oxide layer. Data was analyzed by a linear regression of $D^2 \sim \ln(E_{pulse})$ (1) and damage thresholds together with corresponding beam diameters were obtained. These results of calculated damage thresholds are presented in Tab. 1 and corresponding beam diameters are presented in Tab. 2.

Comparing the values of $F_{th,p}$ for Area 1 in Tab. 1, illustrates the increase in amorphization threshold from 0.226 to 0.267 J/cm^2 going from Si with native oxide layer to Si with a 300 nm SiO_2 layer. Similarly, the threshold of melting increased from 0.408 to 0.486 J/cm^2. Since the damage threshold of SiO_2 is approximately one order of magnitude higher as compared to Si for 1030 nm, 260 fs laser pulses, our measured threshold fluences can only be assigned to silicon damage. Comparing the data with existing work, our amorphization threshold is also in a good agreement with available literature, for the instance of 0.2 J/cm^2 (130 fs, 800 nm) [Bonse 2001].

Si damage threshold [J/cm^2]	$F_{th,p}$ Area 1	$F_{th,p}$ Area 2	$F_{th,p}$ Area 3
native SiO_2 layer	0.226 amorphization	0.334	0.408 melting
300 nm SiO_2 layer	0.267 amorphization	0.486 melting	1.902 sec. crater

Table 1. Damage peak threshold fluences corresponding to modification thresholds of outer edges of Areas 1, 2 and 3 on sample with native and artificial SiO_2 surface layer, calculated for ω_0 = 13.2 µm.

To compare the damage threshold values, one must also keep in mind significant changes of surface reflectivity and therefore deposited or absorbed energy. A SiO_2 layer on silicon surface acts as an antireflection coating. This effect depends on SiO_2 layer thickness and incident wavelength. We consider the refractive indices $n_{air} = 1$, $n_{Si} = 1.450$ [Malitson 1965] and $n_{SiO2} = 3.565$ [Schinke 2015] for wavelength 1030 nm. Applying a simple model of single layer reflectance of transparent film (air-SiO_2-Si) [Heavens 1991], we obtain reflectivity of uncovered silicon $R_{0nm} = 31.6\%$ and $R_{300nm} = 27.3\%$, for silicon with 300 nm SiO_2 layer. Their small 4.3% difference of static reflectivity suggests a decrease of melting threshold; however, contradicts both observed changes. It is also necessary to mention here that reflectivity of the sample surface evolves in time after irradiation and within the picosecond time scale it may change by more than 100% [Rapp 2013].

We also obtained Gaussian beam radiuses ω_0 for both samples and for all investigated areas. These are summarized in Tab. 2 where it can be seen, that for silicon, with native oxide layer, all three measured beam radius values are close, with mutual variation of less than 3%. Whereas the beam radiuses obtained from the sample with 300 nm oxide layer differ significantly, by more than 32%, when compared to each other. Comparing data of threshold fluence values and corresponding spot radiuses, for both kind of samples (Tab. 1 and 2), one can observe that in both cases there is a visible trend of increasing measured ω_0 with increasing threshold fluence of associated modification threshold process. One of the possible reasons for such a trend could be the confinement of deposited pulse energy within the Si-SiO_2 interface, which spreads laterally and seemingly increases the beam spot size.

Furthermore, comparing the spot size measurements on both samples in Tab. 2, only the observed thresholds for the

amorphization region (Area 1) give consistent results. Small deviation of beam radiuses measured for Area 1 may have also been caused by other factors, such as misplacement of the sample or error in the sample focal plane position. Assuming the theoretical spot radius $\omega_0 = \lambda.M^2/\pi.\theta_{div}$ = 12.8 µm (wavelength λ = 1030 nm, M^2 = 1.15 and divergence angle θ_{div} = 0.0294), supports our findings, that the spot size values measured for the lowest observable threshold are close to the theoretically predicted value. Therefore, fluences stated in Fig. 5 and Tab. 1 are based on the ω_0 = 13.2 µm.

beam waist ω_0 [µm]	ω_0 Area 1	ω_0 Area 2	ω_0 Area 3
native SiO_2 layer	13.17 (± 0.04)	13.31 (± 0,04)	13.55 (± 0.05)
300 nm SiO_2 layer	13.65 (± 0.05)	15.2 (± 0.1)	18.0 (± 0.1)

Table 2. Gaussian beam radius parameters ω_0 obtained during evaluation of damage thresholds of areas 1, 2 and 3 on sample with native and artificial SiO_2 surface layer.

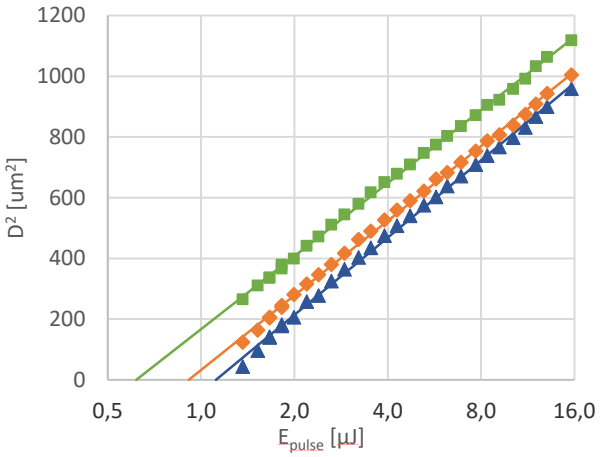

Figure 3. Diameter squared of different modification areas of the silicon surface with native oxide layer: amorphization ■, modification of Area 2 ♦ and melting ▲ as a function of laser pulse energy. Solid lines are linear regressions of the data.

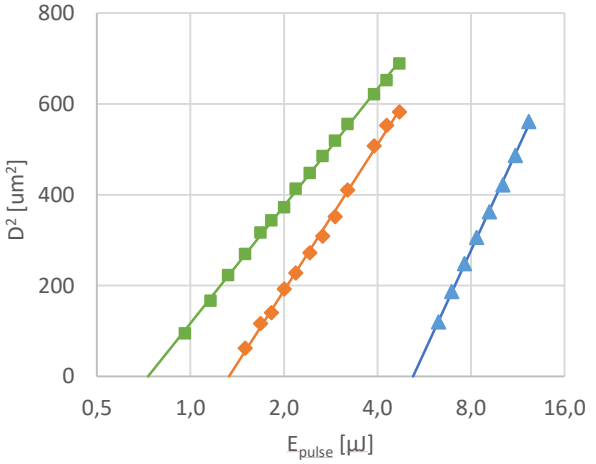

Figure 4. Diameter squared of different modification areas of the silicon surface with 300 nm SiO_2 layer: amorphization ■, melting and oxide layer removal ♦ and secondary crater formation ▲ as a function of laser pulse energy. Solid lines are linear regressions of the data.

3.2 Overview of laser irradiated spot morphology

Fig.1 shows optical micrographs of irradiation spots made on (a) Si with native and (b) Si with 300 nm SiO_2 layer. Several annulus and circular regions can be observed in both images. Each region belongs to a different laser induced modification mechanism. The abrupt change of optical appearance at their borders makes them easily distinguishable. It should be mentioned that in the case of silicon with native oxide layer, the optical contrast between individual regions was the highest in the blue part of optical spectrum. Therefore, blue channels of RGB optical microscope images were evaluated for the damage threshold diameter measurements.

Fig. 5a-h shows SEM images of irradiation spots made on Si sample with 300 nm SiO_2 layer. In order to determine the modification thresholds during selective indirect ablation of the 300 nm SiO_2 layer on Si, the sample was irradiated with laser pulse fluence from 0.35 to 6.5 J/cm^2. Eight unique spot morphologies can be distinguished within this fluence range. Each particular irradiation spot was also further studied by an AFM to obtain spot topography profile. The measured surface profiles of all irradiation spots are given in Fig. 5 below each corresponding SEM spot image.

Our microscopy observations show, that there is no optically observable modification, neither on 300 nm SiO_2 nor on the Si surface below oxide layer, for fluences below 0.37 J/cm^2 (E_p = 1 uJ). Amorphization of silicon surface without any modification of oxide layer can be observed above this fluence value within a short interval of fluences 0.37 – 0.5 J/cm^2 (1 – 1.4 µJ) (see inset of Fig. 5a). For fluences ranging from 0.5 - 0.7 J/cm^2 (1.4 – 1.9 µJ) a single surface blister of SiO_2 on silicon surface was observed (Fig. 5b). This SiO_2 layer delamination and blister formation was also observed within [Rapp 2013, McDonald 2007]. In such studies, the blister formation was described as a highly dynamic process with blister expansion rates of up to 1800 m/s (for 100 nm oxide layer grown on Si surface [Rapp 2013]). This blister formation, according to our understanding, appears to originate from the laser pulse energy absorption by the silicon surface below the SiO_2 layer. The laser energy fluence is too low for multiphoton absorption and damage of SiO_2 [Mirza 2016, Stuart 1996]. Therefore, it is presumed the silicon undergoes melting and vaporization due to laser energy absorption. As the ablation is confined, the pressure of silicon vapor lifts the oxide layer up, perpendicular to the silicon surface and creates a hemispherical blister structure. Following this process, the silicon may recrystallize with many lattice defects [Rublack 2012]. Newton ring patterns, visible in Fig. 1b and inset of Fig. 5b, are caused during optical imaging due to the microscope light interference between the flat Si and inner curved SiO_2 surface within the blister region.

Looking further in Fig. 5c, at higher fluences (0.7 – 1.1 J/cm^2, 1.9 – 3.0 µJ), the hemispherical blister structure changes into a doughnut shaped bulge. From this, we infer that within this fluence range, the hot silicon ablation products may transfer thermal energy to the inner part of oxide layer, leading to layer softening and eventual deformation [Voelkel 2012]. After reaching the maximum bump height of several hundreds of nm [McDonald 2007, Rapp 2013], internal pressure drops due to vapor cooling, and the force of atmospheric pressure pushes the still soft oxide layer back to the silicon surface. The first evidence for SiO_2 layer breaking is visible in the range 1.1 – 1.25 J/cm^2 (3.0-3.4 µJ) (Fig. 5d). This corresponds well with available literature

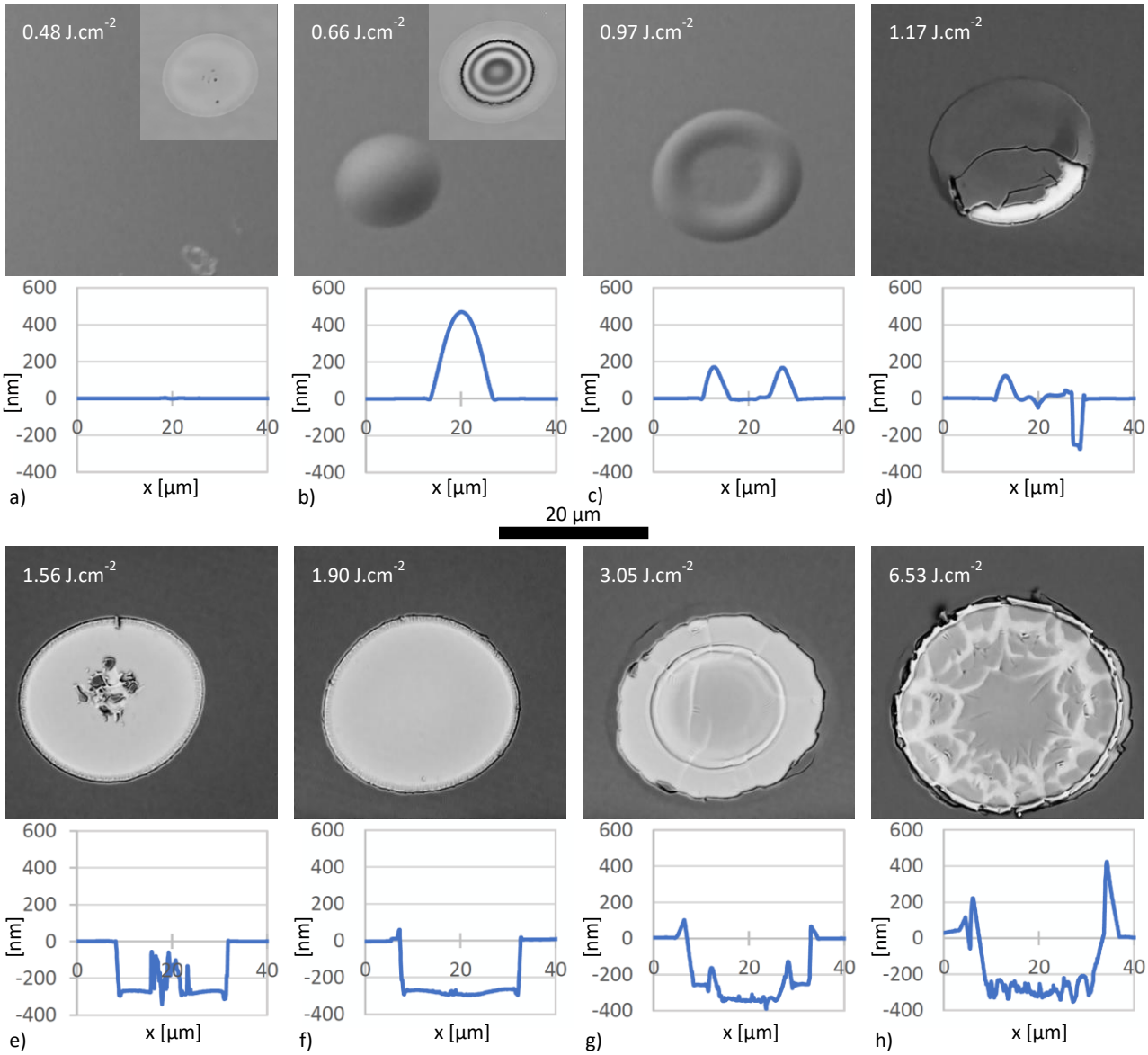

Figure 5. Scanning electron microscope images of silicon with 300 nm SiO_2 layer, demonstrating evolution through different regimes of surface modification with increasing laser fluence from a) to h). Insets in a) and b) show the silicon surface (below SiO_2) imaged by laser scanning confocal microscope. All represented fluences are calculated for a spot radius of 13.2 µm. The corresponding height profiles of irradiation spots are plotted below each SEM micrograph. Zero depth levels correspond to the upper surface of the SiO_2 layer.

by Herman et. al. ($F_{th\ breaking}$ = 1.19 J/cm² for 321 nm of SiO_2, λ = 1064 nm, 8 ps) [Hermann 2010]. A strong damage of the oxide layer is clearly visible in Fig. 5d; however, a substantial part of the layer is still in close contact with underlying silicon. Contrary to expectations, oxide layer breaking starts from the sides of the irradiated spot. At somewhat higher fluences of 1.25 – 1.6 J/cm² (3.4-4.4 µJ) (Fig. 5e) the surface layer is completely ablated, but several pieces of it appear to be redeposited in the central part of the ablation spot. Clean ablation spot with a smooth flat crater bottom, which was the aim of several studies [Herman 2010, Rublack 2012], is achieved in the fluence range of 1.6 – 1.9 J/cm² (4.4 – 5.2 µJ) (Fig. 5f). However, a 1 µm wide region at the side of the opened silicon surface contains quasi-periodic structures from resolidified material (Fig. 5e-f). At even higher fluences (~3 J/cm²), a secondary crater surrounded by a shallow circular rim around the middle part of ablation spot appears (Fig. 5g). Several mechanisms can be responsible for such a crater morphology. First, a massive ablation of solid target should proceed through a phase explosion process (i.e. decay of material into vapor and nanodroplets) [Shugaev 2017]. The pressure of ablation products becomes so high that it may lead to a complete removal of SiO_2 dome. Besides this, Coulomb explosion, rapid atomization and nano-fragmentation of material may exist [Sugioka 2013]. Consequently, the recoil pressure exerted by the ablation products to the molten target surface may lead to formation of these rim structures [Korner 1996]. Such rim structures were also observed for large band gap dielectric materials for fluences much higher than the damage threshold of material [Mirza 2016]. Furthermore, at peak fluence above approximately 3.5 J/cm² (9.5 µJ) damage across the whole spot surface can be observed. The edge of the secondary crater shifts towards the spot margin and transforms its shape into thin unpeeling sheets. The origin of the star-like surface structure is uncertain at this stage.

4 CONCLUSIONS

Modification thresholds of 0.5 mm thick silicon with native and 300 nm thick artificial oxide layer were studied for 260 fs, 1030 nm laser pulses, in order to determine the influence of particular kind of laser induced modification process on the Gaussian beam spot size measurement. The measurement method used was based on the dependence of the modified area diameter on a pulse energy [Liu 1982]. From the variety of complex laser

induced modification process observable within irradiation spot, we choose three modification regions, easily separable from each other. The threshold fluences of two corresponding process for each sample were compared. We relate the first physical process, namely amorphization, with the lowest obtained modification threshold of 0.226 J/cm^2 for silicon with a native oxide layer and 0.267 J/cm^2 for silicon with a 300 nm oxide layer. Similar behavior was observed for an increase in the melting threshold fluence from 0.408 (native SiO_2) to 0.486 J/cm^2 (300 nm SiO_2). Both changes contradict to the 4.3% lower starting static reflectivity of the sample with 300 nm SiO_2.

It was shown that for both studied oxide layers ,the experimental results were closest to the theoretical calculations when a modification process with the lowest threshold fluence was used. For higher fluences, the measured spot size was larger as compared to the theoretical one. This trend is especially valid in regards to 300 nm oxide coating, in which the spot size for the highest measured threshold was 40% larger than the expected theoretical value. On the other hand, the observed increase of the spot size on the sample with native oxide layer was less than 3 %. This gives a hint for all future spot size measurements on how to correctly set the fluence range and evaluate the data. We expect, the above statement may be extended to all other cases of 0.5 mm or thicker materials with surfaces covered by nonabsorbing transparent coating with damage thresholds significantly higher, than the underlying material.

ACKNOWLEDGMENTS

This work was supported by the European Regional Development Fund and the state budget of the Czech Republic (Project No. BIATRI: CZ.02.1.01/0.0/0.0/15_003/0000445), the Ministry of Education, Youth and Sports of the Czech Republic (Programme NPU I Project No. LO1602 and Large Research Infrastructure Project No. LM2015086). J.S. also acknowledges the support of the Grant Agency of the Czech Technical University in Prague (No. SGS16/244/ OHK4/3T/14).

REFERENCES

[Bonse 2001] Bonse, J., et al. Femtosecond laser ablation of silicon–modification thresholds and morphology. Applied Physics A, June 2001, Vol. 74, pp 19-25. DOI 10.1007/s003390100893

[Gnilitskyi 2016] Gnilitskyi, I., et al. Mechanisms of high-regularity periodic structuring of silicon surface by sub-MHz repetition rate ultrashort laser pulses. Applied Physics Letters, October 2016, Vol. 109, DOI 10.1063/1.4963784

[Heavens 1991] Heavens, O. S. Optical properties of thin solid films. New York: Dover Publications, 1991, pp 55-59, ISBN 0-486-66924-6

[Hermann 2009] Hermann, S., et al. Picosecond laser ablation of SiO_2 layers on silicon substrates. Applied Physics A, November 2009, Vol. 99, pp 151-158, DOI 10.1007/s00339-009-5464-z

[Korner 1996] Körner, C., et al. Physical and material aspects in using visible laser pulses of nanosecond duration for ablation. Applied Physics A, February 1996, Vol. 63, pp 123–131, DOI 10.1007/BF01567639

[Liu 1982] Liu, J.M. Simple technique for measurements of pulsed Gaussian-beam spot sizes. Optics letters, May 1982, Vol. 7, No. 5., pp 196-198

[Malitson 1965] Malitson, I. H. Interspecimen comparison of the refractive index of fused silica. Journal of the Optical Society of America, 1965, Vol. 55, pp 1205-1209, DOI 10.1364/JOSA.55.001205

[Mangersnes 2010] Mangersnes, K., et al. Damage free laser ablation of SiO_2 for local contact opening on silicon solar cells using an a-Si:H buffer layer. Journal of Applied Physics, February 2010, Vol. 107, DOI 10.1063/1.3309382

[McDonald 2007] McDonald, J. P., et al. Pump-probe imaging of femtosecond pulsed laser ablation of silicon with thermally grown oxide films. Journal of Applied Physics, September 2007, Vol. 102, DOI 10.1063/1.2778740

[Mirza 2016] Mirza, I., et al. Ultrashort pulse laser ablation of dielectrics: Thresholds, mechanisms, role of breakdown. Scientific Reports, December 2016, Vol. 6, DOI: 10.1038/srep39133

[Rapp 2013] Rapp, S., et al. Physical mechanisms during fs laser ablation of thin SiO_2 films. Physics Procedia, 2013, Vol. 41, pp 734-740, DOI 10.1016/j.phpro.2013.03.141

[Rapp 2014] Rapp, S., et al. The combination of direct and confined laser ablation mechanisms for the selective structuring of thin silicon nitride layers. Physics Procedia, 2014, Vol. 56, pp 998-1006, DOI 10.1016/j.phpro.2014.08.011

[Rublack 2011a] Rublack, T., et al. Laser ablation of silicon dioxide on silicon using femtosecond near infrared laser pulses. Energy Procedia, April 2011, Vol. 8, pp 467-472, DOI 10.1016/j.egypro.2011.06.167

[Rublack 2011b] Rublack, T., et al. Selective ablation of thin SiO_2 layers on silicon substrates by femto- and picosecond laser pulses. Applied Physics A, March 2011, Vol. 103, pp 43-50, DOI 10.1007/s00339-011-6352-x

[Rublack 2012] Rublack, T., et al. Proof of damage-free selective removal of thin dielectric coatings on silicon wafers by irradiation with femtosecond laser pulses. Journal of Applied Physics, July 2012, Vol. 112, DOI 10.1063/1.4739305

[Schinke 2015] Schinke, C., et al. Uncertainty analysis for the coefficient of band-to-band absorption of crystalline silicon. AIP Advances, June 2015, Vol. 5, DOI 10.1063/1.4923379

[Shugaev 2017] Shugaev, M. V., et al. Mechanism of single-pulse ablative generation of laser-induced periodic surface structures. Physical Review B, November 2017, Vol. 96, DOI 10.1103/PhysRevB.96.205429

[Stuart 1996] Stuart, B. C., et al. Nanosecond-to-femtosecond laser-induced breakdown in dielectrics. Physical Review B, January 1996, Vol. 53, pp 1749 - 1761, DOI 10.1103/PhysRevB.53.1749

[Sugioka 2013] Sugioka, K. and Cheng, Y. Ultrafast Laser Processing: From Micro- to Nanoscale. Jenny Stanford Publishing, 2013, pp 99-161, ISBN 9789814267335

[Voelkel 2012] Voelkel, R. Wafer-scale micro-optics fabrication. Advanced Optical Technologies, May 2012, Vol. 1, pp 135-150, DOI: 10.1515/aot-2012-0013

[Zhang 2010] Zhang, J., et al. Determining mean thickness of the oxide layer by mapping the surface of a silicon sphere. Optics Express, March 2010, Vol. 18, pp 7331 - 7339, DOI: 10.1364/OE.18.007331

CONTACTS

Ing. Juraj Sladek
HiLASE Centrum, Institute of Physics CAS, Za Radnici 828, 252 41 Dolni Brezany, Czech Republic
+420 314 007 734, juraj.sladek@hilase.cz